RSC Advances

ROYAL SOCIETY OF CHEMISTRY

www.rsc.org/advances

Journal Name

RSCPublishing

ARTICLE

In vitro effects of differentially shaped hydroxyapatite microparticles on RAW264.7 cell responses

Cite this: DOI: 10.1039/xoxxoooooox

Huijun Zeng, †[a] Hui Yang, †[b] Xinghui Liu, [a] Dandan Shi, [a] Biao Cao, [a] Chang Du, [b] Jun Ouyang, [a] Lei Yu, [a] Yingjun Wang*[b] and Hua Liao*[a]

Received ooth January 2012,
Accepted ooth January 2012

DOI: 10.1039/xoxxoooooox

www.rsc.org/

While numerous reports demonstrated that the properties of hydroxyapatite (HA) particle affects its biological effects, the potential role of particle shape is drawing more and more attention and concern. The present report aims to investigate the effects of microrod and microsphere HA particles on RAW264.7 cell responses *in vitro*. The two shaped HA particles were synthesized with the aids of hydrothermal method and pH regulation, and then characterized by scanning electron microscope (SEM). The cytotoxicity to RAW264.7 cells was assessed on LDH release with HA particle concentrations in 200μg mL^{-1}, 500μg mL^{-1} and 1000μg mL^{-1}. Based on the similar effects among concentrations, 1000μg mL^{-1} concentration was selected for further investigations and Live/Dead staining was then used to observe the cell viability for 24h. Furthermore, particle-cell association and cell apoptosis were detected by Alizarin Red staining and western blot skill, respectively. Cell proliferation was performed by CCK-8 test for 5 days. Moreover, to explore the effects of particle shape on differentiation, RANKL induced RAW264.7 cell osteoclastogenesis was investigated through qRT-PCR analysis on related genes (RANK, TRAP, MMP-9 and CTSK) and the NF-κB signaling genes (IκBα, IKKβ, c-Fos and NFATc1) expressions for 6 days. In the results, we found that microrod and microsphere HA particles had no difference on viability of RAW264.7 cells at the early co-incubation time (within 24h), but microrod particles triggered more striking non-specific cellular uptake or contact with RAW264.7 cells and induced more apoptotic signal. Moreover, compared to microsphere particles, microrod particles initiated more conspicuous proliferation inhibition and interfered with osteoclastic differentiation process profoundly with down-regulation of osteoclastogenesis-related and NF-κB-related gene levels. Our results indicate that the shape-dependent effects of HA particles on cellular response of co-cultured RAW264.7 cells *in vitro*, and may provide more understanding towards the potential role of HA wear debris shapes *in vivo*.

Introduction

It is well known that the natural bone is mainly made up of extracellular matrix proteins and the mineral hydroxyapatite (HA). HA is widely used as bone implant coating or defect filling material in orthopaedic surgery for its good compatibility, bioactivity and bone-bonding properties [1, 2]. However, the HA wear debris production and accumulation due to the aseptic loosening or periprosthetic osteolysis, which further limits the longevity of prosthesis use, should also be taken into consideration [3, 4]. Numerous studies show that periprosthetic osteolysis occurs as a result of biological cellular response to the wear debris and is considered as one of the leading causes of implant failure [5, 6]. Wear debris around prosthesis can induces the macrophages activation with the release of cytokines and growth factors, which further trigger the activation of osteoclasts and ultimately governs the development of osteolysis [7, 8]. In addition, wear debris can also cause recruitment of other cells, such as fibroblasts [3], lymphocytes [9] and osteoblasts [10]. Therefore, the use of synthetic HA as bone substitute calls for the influence on the adjacent cells *in vitro*. Recently, many papers deal with the relationship between the morphology of HA and its biological effects *in vitro* [11-16]. For example, the team of Grandjean-Laquerriere reported the effects of differently shaped micro-sized HA particles (mHAp) on the production of various inflammatory cytokines (e.g., TNF-a, IL-6, IL-18) [11, 12]; Xinxin Zhao et al. demonstrated the shape-dependent effect of HA nanoparticles on cytotoxicity and particle-cell association [13]. However, the study on the effects of particles shape during the resorption of

HA based prosthesis is relative paucity, especially for osteoclastogenesis, and still needed more detailed works.

In this study, the present report aims to investigate the effects of microrod and microsphere HA particles on RAW264.7 cell responses *in vitro*. The two mHAp were synthesized with the aids of hydrothermal method and pH regulation. RAW264.7 cells, a monocyte/macrophage cell line with the capability of differentiating into osteoclasts under the stimulation of soluble RANKL (the receptor activator of nuclear factor-κB ligand), was selected as an *in vitro* inducible osteoclast culturing model and co-cultured with microrod and microsphere particles. The cytotoxicity, cell viability, particle-cell association, apoptosis and proliferation of RAW264.7 cells were detected and compared after exposing cells to the microrod and microsphere particles, as well, the transcriptional levels of the key factors involved in osteoclastogenesis were analyzed, for monitoring events during which wear debris was in contact or reacting with the surrounding biological environment.

Materials and methods

Preparation and characterization of mHAp particles

In this study, analytical grade reagents were used and the two mHAp were synthesized through the hydrothermal method and further modified with pH regulation. The preparation process of mHAp was as follows: 12mM $(NH_4)_2HPO_4$ was added into 60mL de-ionized water. The pH values were adjusted to 6.0 for microsphere particles, or 5.0 for microrod particles, by using 2M HNO_3, respectively. And then, 20mM $Ca(NO_3)_2{\cdot}4H_2O$ was added, and the pH of the mixture was adjusted to 5. 0.9g sodium citrate was added into the solution with vigorous stirring, and then transferred the solution into a Teflon bottle held in a stainless steel autoclave, reacted at 180°C for 2h, cooled naturally. The precipitation was washed with de-ionized, centrifuged, frozen drying for further use. After frozen drying, the two samples were placed in a vacuum coating machine, sprayed and scanned by scanning electron microscope (SEM). For further co-culture with RAW264.7 cells, mHAp were sterilized by autoclave way and added with Dulbecco's Modified Eagle Medium (DMEM) (Hyclone, USA). Prior to incubation, mHAp suspensions were sonicated for 15min using an Ultrasonic Generator.

RAW264.7 cells culture

RAW264.7 cells (murine macrophages-like cell line, ATCC, TIB-71) were cultured in DMEM supplemented with 10% fetal bovine serum (FBS, Hyclone, USA), 100U/mL penicillin, 100μg/mL streptomycin, 2Mm L-glutamine and incubated at 37°C in a 5% CO_2 humidified air incubator (Thermo Scientific HERA Cell 150i, USA). Cells were maintained in 75cm^2 cell culture flasks and passaged upon 70-80% confluence every 2-4 days. Cells with the density of $1\times10^4/cm^2$ were used for further assays.

Cytotoxicity and viability analysis

The cytotoxicity of mHAp on RAW264.7 cells was assessed by lactate dehydrogenase (LDH) cytotoxicity detection kit (Roche Diagnostics, Germany). RAW264.7 cells were plated in 24-well plates (Corning, NY, USA) and treated by the two of mHAp suspensions with final concentrations of 200, 500 and 1000μg mL^{-1} respectively. Cells were treated according to the manufacturer's instruction of the kit after 24h incubation and absorbance was measured at 490nm wavelength (reference, 620nm) using Multiscan Go microplate reader (Thermo Fisher, Finland). Untreated cells were set as the control.

For cell viability evaluation, RAW264.7 cells were cultured on glass coverslips (0.17mm thickness, 14mm diameter), and stained with Live/Dead Viability/Cytotoxicity Kit (Invitrogen, USA). After treating with mHAp suspensions for 24h, cells were washed by PBS and stained by mixture of calcein AM (2μM) and EthD-1 (4μM) for 30min in the absence of light at 37°C. Samples were then observed under the fluorescence microscopy (Olympus BX51, Japan) and images were captured randomly (Olympus DP70, Japan). The number of viable cells was counted by the Image-Pro Plus 6.0 software (Media Cybernetic, Inc.MD, USA) and compared to that of untreated RAW264.7 cells.

Particle-cell association detection

In order to quantify the association between the two mHAp and RAW264.7 cells, Alizarin Red staining (ARS) was adopted in this study. Cells were cultured in six-well plate and treated with two mHAp for 24h. After that, PBS washing (3 times) and paraformaldehyde fixation (30 min) were performed, followed by deionized water washing and Triton X-100 permeating (0.1%, 5 min). The cells were then stained with ARS for 5 min at room temperature (RT) with gentle shaking. After several washes with water and rinsed in PBS to reduce nonspecific ARS staining, the images were obtained under an inverted phase contrast microscope (Olympus, Tokyo, Japan). For particle-cell association analysis, the Image-Pro Plus 6.0 software was performed to quantify the intensity of staining. The integrated optical density (IOD) and area of interest (AOI) of all the positive staining (intense red staining) were measured, respectively. The mean density (IOD/AOI) was then calculated and compared.

Apoptosis and proliferation analysis

To explore cell apoptosis, RAW264.7 cells were cultured and treated with two mHAp for 24h. Cells were washed, stained with Hoechst 33258 for 30 min in 37°C and 5% CO_2 condition, and observed under the fluorescence microscope. Hoechst 33258 is a DNA fluorescent dye probe binding to the minor groove of AT-rich DNA sequence and the Hoechst-DNA combination can emit blue fluorescence through ultraviolet excitation. When cell apoptosis occurred, the nuclei display chromatin condensation or cell shrinkage with bright blue fluorescence, whereas normal cell nuclei are homogeneously with blue fluorescence. Fluorescence intensity of apoptotic cells was calculated through Image-Pro Plus 6.0 software.

For further verifying the effects of two mHAp on RAW264.7 cell apoptosis, the protein levels of Bcl-2, Bax and Caspase-3 were detected using Western Blot skill. After mHAp treatment for 24h, total protein of treated cells was extracted according to the manufacturer's protocol (KeyGEN Bio TECH, China) and protein concentration was measured by a BCA Protein Detection Kit (KeyGEN Bio TECH, China). 40μg total protein was subjected to 10% SDS-poly acrylamide gel electrophoresis for 45 min at 200V and transferred to a PVDF membrane (Millipore Corporation, MA, USA). The membrane were blocked for 1h at RT with 5% nonfat milk (Bio-Red, USA) in Tris-buffered saline containing 0.1% Tween-20 (TBST), and probed with the following antibodies: rabbit polyclonal anti-Bcl-2 antibody (26kDa, 1:1000), anti-Bax antibody (21kDa, 1:1000) (Proteintech, USA) and anti-caspase-3 antibody (17kDa, 1:1000) (Cell Signaling Technology, USA) in 5% nonfat milk in TBST overnight at 4°C. Anti-β-actin antibody (43kDa, 1:1000) (Abcam, USA) was used as a loading control. Subsequently, the blots were washed in TBST three times and incubated with a goat anti-rabbit IgG (H+L) horseradish peroxidase-conjugated secondary antibody (1:5000, Fdbio, China) for 1h at RT. Then washed three times with TBST and visualized using super ECL Plus kit (Pierce, Rockford, USA). The acquired images were then analyzed by Quantity One Software (Bio-Red Laboratories, USA) and the relative protein expression was showed as ratio compared to the internal.

To study cell proliferation, RAW264.7 cells were cultured in 24-well plate and treated with two mHAp. At the day 1, 3 and 5, CCK-8 solution (Dojindo, Japan) with 10% final concentration was added into cell culture and incubated at 37°C for 2h. After delivering the supernatant to 96-well plate (in triplicate for each sample), the absorbance was measured at the wavelength of 450nm under microplate reader, 600nm was taken as reference wavelength.

RANKL induced osteoclastogenesis detection

Firstly, we evaluated *in vitro* morphologic features of RANKL-induced osteoclastogenesis of RAW264.7 cells. Cells were seeded in 6-well culture plates (5×10^4 cells/well) and treated with two mHAp in the presence or absence of 50ng mL^{-1} recombinant mouse RANKL (Sigma-Aldrich, Germany). On day 6, cells were washed, fixed and stained with tartrate-resistant acid phosphatase (TRAP) staining reagent (Sigma, Germany) 1h at 37°C in the dark, followed by nucleus counterstaining using hematoxylin. Cells with more than three nuclei were regarded as TRAP-positive mature osteoclasts. Image-Pro Plus 6.0 software was used to analyze quantitative difference of the number and area of osteoclasts treated or untreated with mHAp.

Quantitative RT-PCR was then applied to investigate transcriptional changes of osteoclastogenesis-related genes in mHAp-treated or untreated RAW264.7 cells, which were induced by RANKL in advance. Total RNA was extracted by TRIzol Reagent (Invitrogen, USA) and the absorbance was measured at 260nm and 280nm. 1μg total RNA was subjected to the synthesis of cDNA by using RevertAid First Strand cDNA Synthesis Kit (Thermo Scientific, Germany). Reactions were initiated by incubation at 65°C for 5 min, followed by 60 min at 42°C and terminated the reaction by heating at 70°C for 5 min. The cDNA performed to PCR by using the Maxima SYBR Green/ROX qPCR Master Mix (Thermo Scientific, Germany). 25μl total reaction volume included 12.5μl Mix (2X), 1.5μl (10mM) primers (Table1) synthesized by Sangon Biological Engineering Technology and Services Co., Ltd (Shanghai , China), 8.5μl nuclease-free water and 0.8μg/1μl cDNA. PCR reaction was run in SteponePlus Real-Time PCR system (Applied Biosystems, Germany) and analyzed using Stepone software. The qPCR protocol contained initial denaturation at 95°C 10 min, then 40 cycles including 95°C for 5s denaturation, 60°C for 30s annealing and 72°C for 30s extension. All experiments were performed in triplicate, and the specificity of the PCR products was verified with melting curve analysis. The amount of each respective amplification product was determined relative to the house-keeping gene β-actin. The fold change in gene expression relative to control was calculated by $2^{-\Delta\Delta CT}$.

Statistical analysis

Results were represented as mean ± standard deviation (SD) for three separate experiments. Statistical data were analyzed by SPSS 13.0 software and statistical differences were assessed by one-way analysis of variance (ANOVA), followed by a post hoc Tukey's Test. Value of $P<0.05$ was considered as statistical significant.

Table 1

Primer sequences used for quantitative RT-PCR

mRNA	Forward (F) and Reverse (R) Primer sequence(5'-3')	Gene Bank Acc
RANK	F:ATCCAGCAGGGAAGCAAA R:GGGACACGGGCATAGAGT	NM_009399
TRAP	F:ACGGCTACTTGCGGTTTCA R:TCCTTGGGAGGCTGGTCTT	NM_001102405.1
MMP-9	F:TAGGGCTCCTTCTTTGCTT R:CCACTCCTTCCCAGTCTCT	NM_013599.2
CTSK	F:CTGCGGCATTACCAACAT R:CACTGGAAGCACCAACGA	NM_007802.3
IκB α	F:ATGGAAGTCATTGGTCAGGTG R:GGCAAGATGTAGAGGGGTATTT	NM_010907.2
IKK β	F:TGGCCTTCGAGTGCAT R:GGGAAGGGTAGCGAACTT	NM_010546.2
c-Fos	F:CGAAGGGAACGGAATAAGA R:CTGGGAAGCCAAGGTCAT	NM_010234.2
NFATc1	F:GTCTCACCACAGGGCTCACT R:ATGGCTCGCATGTTATTTTC	NM_001164112.1
β-actin	F:GGTCATCACTATTGGCAACG R:TCCATACCCAAGAAGGAAGG	NM_007393.3

Results

Characterization of microrod and microsphere HA particles

The two shaped mHAp were characterized by using field emission scanning electron microscope system (SEM, Nova NanoSEM 430, Netherlands) and demonstrated in Fig.1.

Results revealed that the synthesized microrod and microsphere HA particles were homogeneous in shape, respectively. The particle length (microrod, Fig.1A) or particle diameter (microsphere, Fig.1B) was similar in size, which ranged from 1-3μm.

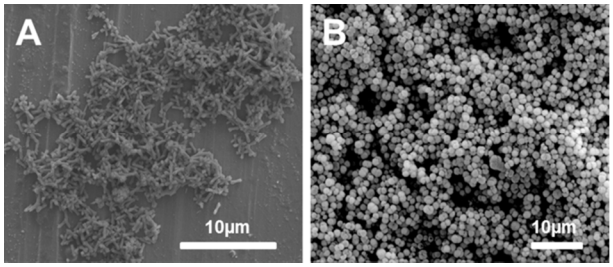

Fig.1 Scanning electron microscope images of microrod (A) and microsphere (B) HA particles.

Two mHAp have no influence on RAW264.7 cells viability at early treating time

Since cytotoxicity assay is one of the most common ways to evaluate cell viability, we firstly explored whether mHAp influence cytotoxicity of RAW264.7 cells within 24h *in vitro*. Cells were incubated with various concentrations of two mHAp (200, 500, and 1000μg mL^{-1}) and conducted to LDH assay after 24h co-culturing. Fig.2A showed that the microrod and microsphere HA particles did not show any toxicity to RAW264.7 cells, because the same viability values were measured among two particles-treated cells, as untreated cells, no matter of particle concentration. According to previous studies, a relative high concentration of HA particles was applied to simulate the *in vivo* periprosthetic wear debris study [3, 4, 14, 15], therefore 1000μg mL^{-1} concentration was selected in our study for further investigations. Using Live/Dead viability staining and viable cell counting, we further validated that, there was no difference of viable cell number between two mHAp co-cultured cells during 24h treating, even particle concentration up to 1000μg mL^{-1} (Fig.2B-E). This finding is consistent with the previous suggestion that synthetic hydroxyapatite is biocompatible *in vitro* [1, 16].

The shape of mHAp affects particle-cell association of RAW264.7 cells

To address the role of mHAp shape on cellular internalization, we next detected particle-cell association of RAW264.7 cells to microrod and microsphere HA particles through ARS assay, which binds selectively to calcium salts and is widely used for mineral histochemistry and used to judge calcium uptake of different cells [17]. Cells were co-cultured about 24h with two particles, and then performed ARS assay. As expected, we did not observed red calcium staining in untreated cells (Fig.3A), on the contrary, intensive calcium staining appeared in two mHAp-treated cells (Fig.3B,C). Interestingly, we found ARS density value of microrod particles-treated cells was almost the double of microsphere ones (Fig.3D). Summarily, our results suggest the shape of mHAp has a significant impact on cellular internalization, and RAW264.7 cells readily internalize or contact with microrod HA particles.

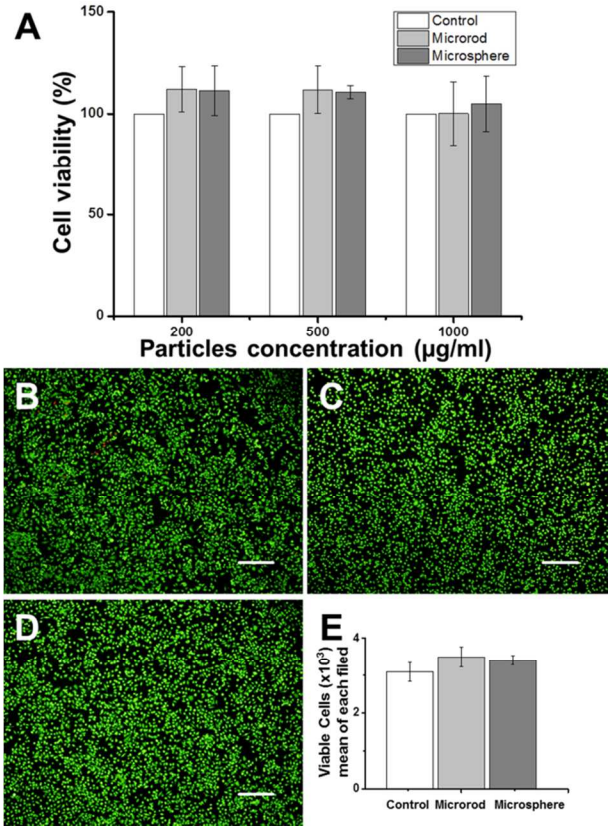

Fig.2 Viability analysis of RAW264.7 cells co-culturing 24h with microrod or microsphere HA particles. Cells were treated with mHAps in different concentrations, and monitored cell viability using LDH assay (A). Live-Dead Staining results of mHAps-treated RAW264.7 cells in 1000μg mL^{-1} concentration were showed as: B, Untreated cells; C, microrod particle-treated cells; D, microsphere particle-treated cells. The number of viable cells was counted and compared (E). Data represent mean ± SD (*n*=3). Scale bar represents 200μm.

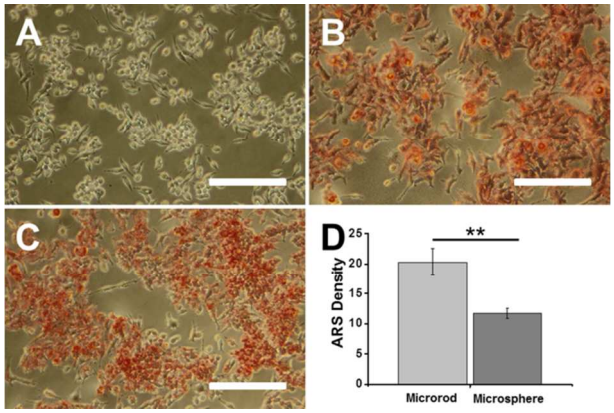

Fig.3 Alizarin Red Staining for RAW264.7 cells co-culturing 24h with microrod and microsphere HA particles. (A), Untreated cells. (B), Microrod particles-treated cells. (C), Microsphere particles-treated cells. (D), the mean ARS density value analysis. Data represent means ± SD (*n*=3). Significance was calculated using one-way ANOVA (**P<0.01). Scale bar represents 200μm.

Microrod particles exhibit obvious cell apoptosis up-regulation and proliferation inhibition

In order to delineate the role of mHAp shape on apoptosis of RAW264.7 cells, we next performed Hoechst 33258 staining on RAW264.7 cells after 24h co-culturing. Under the fluorescence microscope, apoptosis cells exhibited more bright blue color than normal cells. We found the number of apoptotic cells increased if RAW264.7 cells were treated with mHAp, compared to untreated cells (Fig.4A, B, C). The relative fluorescence intensity analysis further revealed that, apoptosis rate of microrod particles-treated cells was higher than microsphere ones while there was no significant significance (Fig.4D). Bcl-2 and Bax are anti- and pro-apoptotic members in BCL-2 family, which regulate and contribute to apoptosis process [18, 19]. Caspase-3 is another key pro-apoptotic protein involved in the activation cascade of caspases responsible for apoptosis execution [20]. We further examined the effect of two mHAp on the protein expression of those key apoptotic signal molecules in 24h co-cultured RAW264.7 cells using western blot. The result demonstrated that, relative protein level of Bcl-2 was significantly decreased in microrod particles-treated cells, than untreated and microsphere particles-treated cells (Fig.4E, F). Comparing to microsphere particles-treated cells, caspase-3 level was slightly increased in microrod particle treated-cells, but has no significant difference (Fig.4E, F). We did not found significant changes of Bax level in two particles-treated cells (data not shown). Together, this initial result suggests microrod particles initiate apoptosis of RAW264.7 cells more readily.

At the 24h co-culturing, we did not find difference of cell viability between two particles-treated cells, however, we detected increased apoptotic cells, and changed protein level of apoptotic molecules in RAW264.7 cells at this time point. It is possible that cell growth was influenced by particles treatment with the prolonged culturing time. Therefore, the WST-8 binding test was used to further address RAW264.7 cell proliferation at the day 1, 3, 5 of co-culturing separately. As shown in Fig.5, untreated cells proliferated quickly with the prolonged culture time (up to 5 days). At the d1, particles treated-cells survived well, with the same proliferation rate as untreated cells. However, we detected cell proliferation inhibition at the day 3 and 5 after two mHAp treatments. At the day 5, proliferation rate of microrod particles-treated cells decreased significantly, than untreated and microsphere particles-treated cells. Those data strongly suggested that, RAW264.7 cells response to microrod particles more sensitive. A possible explanation for this phenomenon is that, microrod particles treated-cells uptake or associate with more calcium particles, and prompt the initiation of apoptosis signals, finally interfere with cell growth and proliferation.

The shape of mHAp affects RANKL-induced osteoclastogenesis in RAW264.7 cells

Our results so far have demonstrated that microrod particles induce more obvious cell apoptosis and proliferation inhibition, than microsphere particles. We next test whether two particles contribute to the differentiation of RAW264.7 cells. We therefore focused on the effects of mHAp on RANKL-induced osteoclastogenesis in co-cultured cells. TRAP staining was

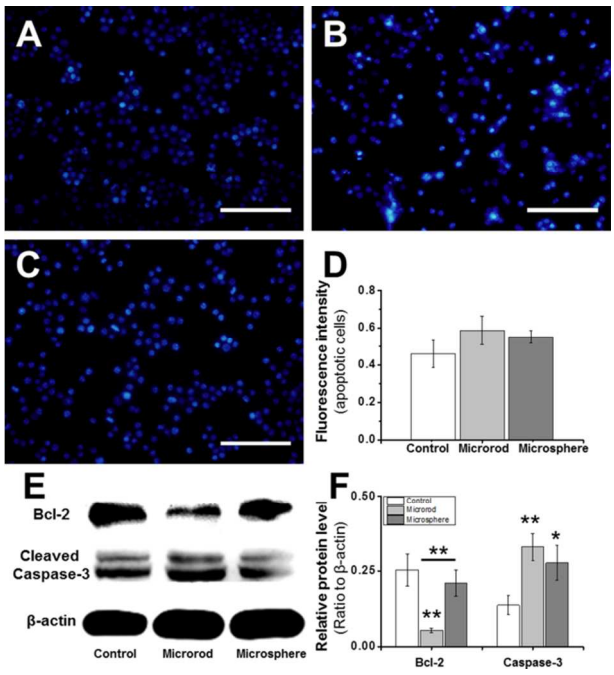

Fig.4 Effects of mHAp on RAW264.7 cell apoptosis were discriminated by Hoechst 33258 staining and western blot analysis. Fluorescent micrographs of RAW264.7 cells, co-cultured 24h with microrod or microsphere particles and stained with Hoechst 33258, were demonstrated. A, untreated cells; B, microrod particles-treated cells; C, microsphere particles-treated cells. D, The relative fluorescence intensity of apoptotic cells. E, Western blot analysis showing the levels of apoptotic proteins (Bcl-2, Caspas-3). F, The relative band intensities from western blots experiments were normalized to the level of β-actin. Data represent means ± SD (n=3). Significance was calculated using one-way ANOVA (vs. control *P<0.05, **P<0.01). Scale bar represents 100μm.

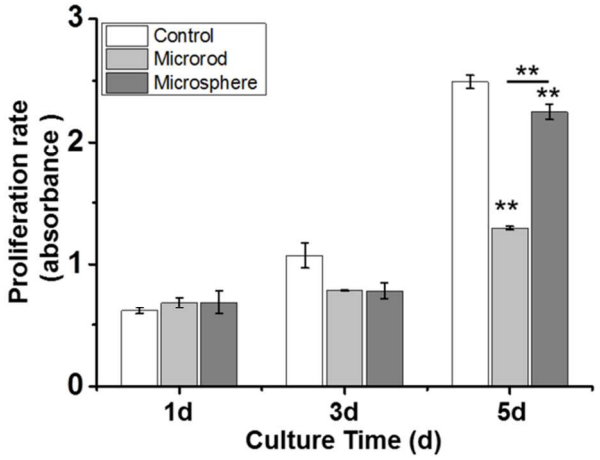

Fig.5 Proliferaion analysis of RAW264.7 cells treated with microrod or microsphere HA particles. Data represent means ± SD (n=3). Significance was calculated using one-way ANOVA (vs. control *P<0.05, **P<0.01).

firstly applied to evaluate morphologic changes of RAW264.7 cells cultured in the presence of RANKL for 6 days with or without mHAp treatment. As expected, $TRAP^+$ multinucleated cells were found with high quantity in two mHAp-treated cells

after RANKL inducing (Fig.6B, C, D), but not in untreated cells (Fig.6A), which received only growth medium. For number and area analysis of differentiated cells (osteoclast-like), no significant difference was found between two particles (Fig.6E, F).

After RANKL stimulation, the RAW264.7 cells *in vitro* will up-regulate osteoclastogenesis-related genes, such as RANK, TRAP, MMP-9 and CTSK [21-23]. We therefore detected and compared the levels of above genes in RANKL-induced cells treated with or without mHAp respectively. qRT-PCR result showed that, mRNA levels of RANK, TRAP, MMP-9 and CTSK were significantly up-regulated in cells treated with RANKL alone (positive control), at the day 3 and 6, compared to untreated control cells (negative control). For mHAp-treated cells, the levels of above osteoclastogenesis-related genes significantly lower than positive control cells, despite the levels of most genes significantly higher than negative control cells. Of notes, RANK， TRAP and MMP-9 levels in microrod particles-treated cells were lower than that of microsphere particles-treated cells at the day 3 and 6, except for CTSK at day 3 (Fig.7).

It has been reported that the application of RANKL rapidly activates NF-κB signaling pathways in RAW264.7 cells [24, 25]. To definitely verify mHAp participate in the inhibition of cell osteoclastogenesis, we compared NF-κB signaling genes levels (IκB α, IKK β, c-Fos and NFATc1). We found mRNA levels of IKK β, c-Fos and NFATc1 were significantly decreased in mHAp-treated cells compared to positive control cells at the day 3 and 6. In addition, at the early treating time (day 3), microrod particles demonstrated significant expression inhibition of c-Fos and NFATc1, than microsphere particles (Fig.7). Thus, our data suggest that, the shape of mHAp, especially for microrod particles, has a role on the inhibition of RANKL-induced RAW264.7 cells osteoclastogenesis *in vitro*.

Discussion

Periprosthetic osteolysis and subsequent aseptic loosening are the most frequent complications in orthopaedic implants [26, 27], which may result from the biological cellular response to wear debris from implant based materials. There is a wealth of evidence that the presence and activation of macrophages, which stimulated by wear debris at the bone-implant interface, closely associated with the periprosthetic osteolysis [28, 29]. Recent understanding indicates that bone marrow-derived macrophages may play a dual role in this osteolysis process, which firstly acts as the major cell in host defense responding to wear debris and secondly as precursors for the osteoclasts responsible for bone resorption [7]. In this study, RAW264.7 cells, an immortalized mouse macrophage cell line, which is the first cell type to respond to foreign bodies like HA wear debris and the precursor cell to differentiate into mature osteoclast, were chosen as the cell model and co-cultured with the microrod and microsphere HA particles *in vitro*. Since the widely use of synthetic HA as bone substitute, the *in vitro* studies were investigated extensively and showed that the shape of HA particles has significant effects on cellular biological responses, involving the production of inflammatory cytokines, the generation of reactive oxygen species, the cytotoxicity and

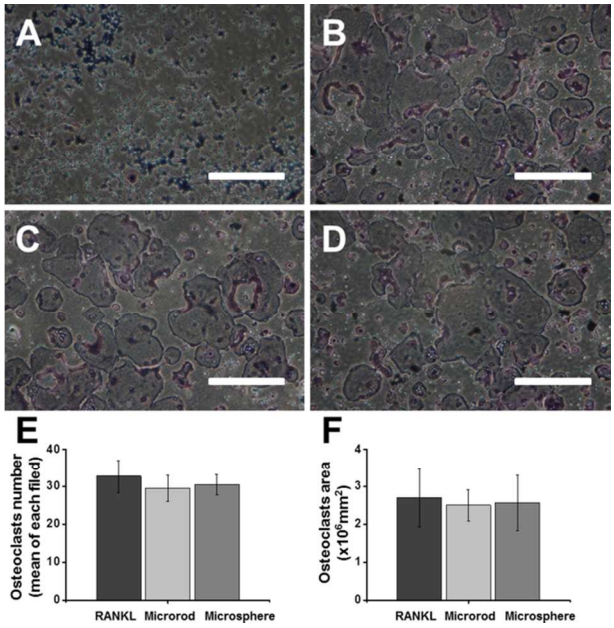

Fig.6 TRAP staining results of RAW264.7 cells following mHAp treatments. Microscope images of stained cells were demonstrated as: A, untreated cells; B, cells treated with RANKL; C, cells treated with microrod particles and RANKL; D, cells treated with microsphere particles and RANKL. The number (E) and area (F) of $TRAP^+$ cells (osteoclast-like) were analyzed using one-way ANOVA. Data represent means ± SD (*n*=3). Scale bar represents 200μm.

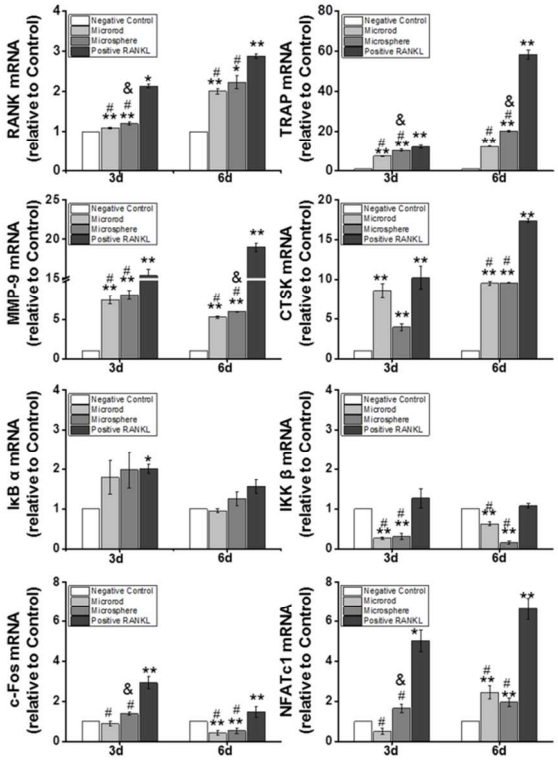

Fig.7 mRNA levels corresponding to osteoclastogenesis-related genes (RANK, TRAP, MMP-9, CTSK) and NF-κB pathway-related genes (IκB α, IKK β, c-Fos, NFATc1) were quantified by qRT-PCR analysis in mHAp-treated cells with or without RANKL stimulation. All data are presented as mean ± SD (n=3). Significance was calculated using one-way ANOVA (vs. Negative Control *P<0.05, **P<0.01, vs. RANKL positive $^{\#}$ P<0.05, vs Microrod $^{\&}$ P<0.05).

proliferation of co-incubated cells, et al [11-13, 30-32]. In spite of these studies, it is still need more detailed work to elucidate the shape-dependent effects of HA particles on special cellular biological activities. Herein, we tested in-depth the hypothesis that the shape of particles has a potential role on altering the cell viability, proliferation, apoptosis, and osteoclastogenesis of co-cultured RAW264.7 cells.

Previous studies have demonstrated that synthetic HA particles exhibits excellent biocompatibility with several cell types *in vitro*, including mesenchymal stem cells (MSCs), osteoblast-like cells, cancer cells etc [33-35]. The studies reported here evaluated firstly the effect of two shaped particles on RAW264.7 cells at the early co-incubation time (within 24h), for determining the susceptibility of this macrophage cell line to two mHAp. The LDH assay and Live/Dead viability staining suggested that the shape of mHAp had no influence on viability of RAW264.7 cells. Even elevating mHAp concentration to 1000μg mL^{-1}, microrod and microsphere HA treated cells still grew well and displayed the same viability as untreated cells (Fig.2). However, when we investigated the association between the two mHAp and RAW264.7 cells within 24h co-culturing, we found microrod particles is more easy to be uptaken by or contact with RAW264.7 cells, because the more intensive calcium staining occurred in microrod particles treated-cells, than in microsphere treated ones. Researchers tend to believe that particle shape-dependent changes of cellular behavior may be rooted in the sensitivity of non-specific cell receptors to different shaped particles [13, 36, 37]. For macrophage, a series of intracellular responses, including apoptosis signal will be triggered after large amounts of calcium salts uptake [38]. Our Hoechst 33258 staining and apoptotic protein analysis verified that, microrod particles-treated cells were more susceptible for apoptotic signal, and triggered conspicuous cell apoptosis (Fig.3). From the above data, we propose the different mHAp shape-dependent changes of cellular behavior happened at the early co-incubation time, which further triggers the different degree of cell apoptosis (Fig.4). Despite of the similar cellular viability between two mHAp treated-cells at the 24h co-culturing, this earlier apoptosis signal initiation implicated cellular viability maybe gradually changed with the prolonged co-incubation time. To test this speculation, we prolonged co-culture time until five days and detected the proliferation of RAW264.7 cells *in vitro*. Results showed that the two mHAp inhibit cell proliferation at the day 3 and 5, especially for microrod particles, which further suggests particle shape have a role on cell reaction and activity (Fig.5) [14].

Since the macrophages can act as precursors for the osteoclasts responsible for bone resorption, we speculated that wear debris with different shapes maybe lead to the functional difference of osteolysis *in vivo*. For osteolysis at the bone-implant interface, osteoblast interaction with particulate wear debris is a key event. Stimulated osteoblast release soluble RANKL, activate NF-κB signaling pathway, and finally help to initiate localized bone resorption [7, 39, 40]. To verify this hypothesis *in vitro*, we further explored the shape-dependent effects of mHAp on osteoclastogenesis of co-cultured RAW264.7 cells. The results from qRT-PCR suggested negative effects of two mHAp on RANKL induced osteoclastogenesis in co-cultured cells, because we detected mRNA levels of RANK, TRAP, MMP-9 genes significantly down-regulated in mHAp-treated cells, compared to untreated but RANKL induced cells. Interesting, the more conspicuous osteoclastogenesis inhibition was observed for microrod particles-treated cells (Fig.7). Because NF-κB signaling pathway can be rapidly activated after RANKL stimulation in osteoclasts [41], we further investigated gene levels of this pathway in mHAp-treated cells. As expected, our result showed that microrod particles significantly down-regulated mRNA levels of c-Fos and NFATc1, the key molecules of NF-κB pathway, at the day 3 of co-culturing, than that of microsphere particles (Fig.7). Though our results were inconsistent to the previous studies on titanium [42] or ultra-high molecular weight polyethylene (UHMWPE) [7] particle-induced osteoclastogenesis, we reported here that the mHAp interfere with the osteolysis process and the shape of particles has a potential role during this process *in vitro*. Compared to wear particle-induced osteolysis model *in vivo*, we speculated that the interference in our study probably due to the relative dense particles in culture medium and the unstable co-cultured environment that lead to reverse impacts on osteoclastogenesis. In addition, the difficulties in generating HA particles with similar size and shape to clinical wear particles may also contribute to these reverse results. However, as to the microsphere particles, the microrod particles initiated obvious cell apoptosis, proliferation and differentiation inhibitions in our study. We suspected this difference caused by shape-effects may root in the different calcium level through the different amount of particle uptake or internalization, but the related mechanism still needs more investigations.

Conclusions

In summary, this study tests the shape-dependent effects of mHAp on cellular response of co-cultured RAW264.7 cells *in vitro*. Comparing to microsphere particles, microrod particles exhibit a higher degree of particle-cell association, which promote apoptosis, inhibit proliferation and osteoclastogensis of RAW264.7. Moreover, this study may suggest that HA wear debris with different shapes *in vivo* contribute to the functional difference of osteolysis. Therefore special attention should be paid for the potential role of particle shapes degraded from the HA based materials for clinical application.

Acknowledgements

This work was supported by the National Basic Research Program of China (Grant no. 2012CB619100), the National Natural Science Foundation of China (Grant no.81171724 and Grant no.81371924) and the China 863 Project (Grant no.2012AA020504).

Notes and references

[a] Department of Anatomy, Key Laboratory of Construction and Detection of Guangdong Province, Southern Medical University, Guangzhou, 510515, China. E-mail: hua-liao@163.com; Fax: +86-20-61648202
[b] School of Materials Science and Engineering, South China University of Technology, Guangzhou, 510641, China.

†The first two authors contributed equally to this work.

*Corresponding authors

1 H. Zhou and J. Lee, Acta Biomater, 2011, **7**, 2769-2781.
2 T. Matsumoto, M. Okazaki, A. Nakahira, J. Sasaki, H. Egusa and T. Sohmura, Curr Med Chem, 2007, **14**, 2726-2733.
3 J. S. Sun, Y. H. Tsuang, W. H. Chang, J. Li, H. C. Liu and F. H. Lin, Biomaterials, 1997, **18**, 683-690.
4 J. S. Sun, F. H. Lin, T. Y. Hung, Y. H. Tsuang, W. H. Chang and H. C. Liu, J Biomed Mater Res, 1999, **45**, 311-321.
5 D. P. Pioletti and A. Kottelat, Biomaterials, 2004, **25**, 5803-5808.
6 Y. Abu-Amer, I. Darwech and J. C. Clohisy, Arthritis Res Ther, 2007, **9 Suppl 1**, S6.
7 E. Ingham and J. Fisher, Biomaterials, 2005, **26**, 1271-1286.
8 W. J. Boyle, W. S. Simonet and D. L. Lacey, Nature, 2003, **423**, 337-342.
9 H. G. Willert, G. H. Buchhorn, A. Fayyazi, R. Flury, M. Windler, G. Koster and C. H. Lohmann, J Bone Joint Surg Am, 2005, **87**, 28-36.
10 J. S. Sun, H. C. Liu, W. H. Chang, J. Li, F. H. Lin and H. C. Tai, J Biomed Mater Res, 1998, **39**, 390-397.
11 P. Laquerriere, A. Grandjean-Laquerriere, E. Jallot, G. Balossier, P. Frayssinet and M. Guenounou, Biomaterials, 2003, **24**, 2739-2747.
12 A. Grandjean-Laquerriere, P. Laquerriere, M. Guenounou, D. Laurent-Maquin and T. M. Phillips, Biomaterials, 2005, **26**, 2361-2369.
13 X. Zhao, S. Ng, B. C. Heng, J. Guo, L. Ma, T. T. Tan, K. W. Ng and S. C. Loo, Arch Toxicol, 2013, **87**, 1037-1052.
14 J. L. Xu, K. A. Khor, J. J. Sui, J. H. Zhang and W. N. Chen, Biomaterials, 2009, **30**, 5385-5391.
15 J. Scheel, S. Weimans, A. Thiemann, E. Heisler and M. Hermann, Toxicol In Vitro, 2009, **23**, 531-538.
16 H. Wang, Y. Li, Y. Zuo, J. Li, S. Ma and L. Cheng, Biomaterials, 2007, **28**, 3338-3348.
17 X. Zhao, B. C. Heng, S. Xiong, J. Guo, T. T. Tan, F. Y. Boey, K. W. Ng and J. S. Loo, Nanotoxicology, 2011, **5**, 182-194.
18 T. G. Cotter, Nat Rev Cancer, 2009, **9**, 501-507.
19 S. Willis, C. L. Day, M. G. Hinds and D. C. Huang, J Cell Sci, 2003, **116**, 4053-4056.
20 I. Budihardjo, H. Oliver, M. Lutter, X. Luo and X. Wang, Annu Rev Cell Dev Biol, 1999, **15**, 269-290.
21 W. Yoon, K. Kim, S. Heo, S. Han, J. Kim, Y. Ko, H. Kang and E. Yoo, Biochem Bioph Res Co, 2013, **434**, 892-897.
22 Y. Y. Kong, U. Feige, I. Sarosi, B. Bolon, A. Tafuri, S. Morony, C. Capparelli, J. Li, R. Elliott, S. McCabe, T. Wong, G. Campagnuolo, E. Moran, E. R. Bogoch, Van G, L. T. Nguyen, P. S. Ohashi, D. L. Lacey, E. Fish, W. J. Boyle and J. M. Penninger, Nature, 1999, **402**, 304-309.
23 M. T. Engsig, Q. J. Chen, T. H. Vu, A. C. Pedersen, B. Therkidsen, L. R. Lund, K. Henriksen, T. Lenhard, N. T. Foged, Z. Werb and J. M. Delaisse, J Cell Biol, 2000, **151**, 879-889.
24 K. Wu, T. H. Lin, H. C. Liou, D. H. Lu, Y. R. Chen, W. M. Fu and R. S. Yang, Osteoporos Int, 2013, **24**, 2201-2214.
25 B. Sung, A. Murakami, B. O. Oyajobi and B. B. Aggarwal, Cancer Res, 2009, **69**, 1477-1484.
26 G. Holt, C. Murnaghan, J. Reilly and R. M. Meek, Clin Orthop Relat Res, 2007, **460**, 240-252.
27 Y. Jiang, T. Jia, P. H. Wooley and S. Y. Yang, Acta Orthop Belg, 2013, **79**, 1-9.
28 M. J. Archibeck, J. J. Jacobs, K. A. Roebuck and T. T. Glant, Instr Course Lect, 2001, **50**, 185-195.
29 E. Ingham and J. Fisher, Proc Inst Mech Eng H, 2000, **214**, 21-37.
30 B. C. Heng, X. Zhao, E. C. Tan, N. Khamis, A. Assodani, S. Xiong, C. Ruedl, K. W. Ng and J. S. Loo, Arch Toxicol, 2011, **85**, 1517-1528.
31 Y. Liu, R. Shelton, U. Gbureck and J. Barralet, J Biomed Mater Res A, 2009, **90**, 972-980.
32 X. Liu, M. Zhao, J. Lu, J. Ma, J. Wei and S. Wei, Int J Nanomedicine, 2012, **7**, 1239-1250.
33 A. Tautzenberger, S. Lorenz, L. Kreja, A. Zeller, A. Musyanovych, H. Schrezenmeier, K. Landfester, V. Mailander and A. Ignatius, Biomaterials, 2010, **31**, 2064-2071.
34 F. Qiang, M. N. Rahaman, Z. Nai, H. Wenhai, W. Deping, Z. Liying and L. Haifeng, J Biomater Appl, 2008, **23**, 37-50.
35 X. Guo, J. E. Gough, P. Xiao, J. Liu and Z. Shen, J Biomed Mater Res A, 2007, **82**, 1022-1032.
36 S. E. Gratton, P. A. Ropp, P. D. Pohlhaus, J. C. Luft, V. J. Madden, M. E. Napier and J. M. DeSimone, Proc Natl Acad Sci U S A, 2008, **105**, 11613-11618.
37 M. Motskin, D. M. Wright, K. Muller, N. Kyle, T. G. Gard, A. E. Porter and J. N. Skepper, Biomaterials, 2009, **30**, 3307-3317.
38 S. Orrenius, B. Zhivotovsky and P. Nicotera, Nat Rev Mol Cell Biol, 2003, **4**, 552-565.
39 D. Granchi, I. Amato, L. Battistelli, G. Ciapetti, S. Pagani, S. Avnet, N. Baldini and A. Giunti, Biomaterials, 2005, **26**, 2371-2379.
40 M. Asagiri and H. Takayanagi, Bone, 2007, **40**, 251-264.
41 J. C. Clohisy, E. Frazier, T. Hirayama and Y. Abu-Amer, J Orthop Res, 2003, **21**, 202-212.
42 F. Liu, Z. Zhu, Y. Mao, M. Liu, T. Tang and S. Qiu, Biomaterials, 2009, **30**, 1756-1762.

We test *in vitro* effects of differentially shaped hydroxyapatite microparticles on RAW264.7 cell responses, which may provide more understanding towards the potential role of HA wear debris shapes *in vivo*.